AD-A077 178 FEDERAL ELECTRIC CORP VANDENBERG AFB CA PERFORMANCE --ETC F/G 17/9
RANGE VERNIER.(U)
AUG 79 R ROY F04703-77-C-0111
UNCLASSIFIED PA300-T-39-32 SAMTEC-TR-79-2 NL

1 OF 1
ADA 077178

END
DATE FILMED
12-79
DDC

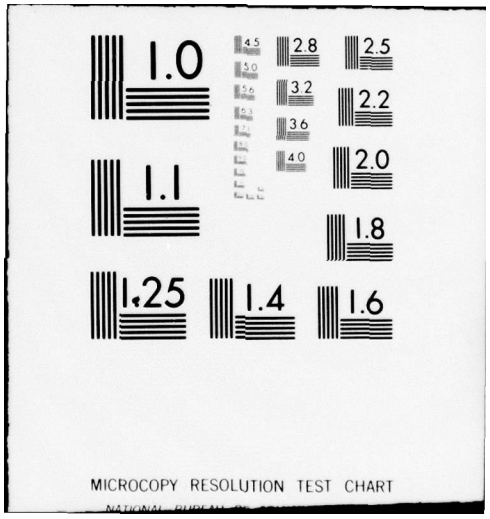
1.0
1.1
1.25
1.4
1.6
1.8
2.0
2.2
2.5
2.8
3.2
3.6
4.0
4.5
5.0
5.6
MICROCOPY RESOLUTION TEST CHART

SAMTEC TR79-2

LEVEL II

12

RANGE VERNIER

AD A077178

DDC
RECEIVED
NOV 23 1979
E

Russell Roy

PERFORMANCE ANALYSIS DEPARTMENT

FEDERAL ELECTRIC CORPORATION
WTR DIVISION, VANDENBERG AFB, CALIFORNIA 93437

AUGUST 1979
FINAL REPORT

APPROVED FOR PUBLIC RELEASE
UNLIMITED DISTRIBUTION

DDC FILE COPY

PREPARED FOR

SPACE AND MISSILE TEST CENTER (AFSC)

VANDENBERG AFB, CALIFORNIA 93437

79 11 21 106

This final report was submitted by Federal Electric Corporation, Vandenberg AFB, CA 93437 under Contract F04703-77-C-0111 with the Space and Missile Test Center, Vandenberg AFB, CA 93437. Operations Research Analyst, Mr. J. McConnell, XRQR, was the Division Project Engineer-in-Charge.

This report has been reviewed by the Information Office (OI) and is releasable to the National Technical Information Service (NTIS). At NTIS, it will be available to the general public, including foreign nations.

This technical report has been reviewed and is approved for publication.

John B. McConnell GS-13
Project Engineer

Kingston A. George GS-14
Chief, Requirements Branch

FOR THE COMMANDER

ROGER D. ROTHWELL, Colonel, USAF
Director of Plans, Programs &
Resources

UNCLASSIFIED

SECURITY CLASSIFICATION OF THIS PAGE *(When Data Entered)*

REPORT DOCUMENTATION PAGE	READ INSTRUCTIONS BEFORE COMPLETING FORM
1. REPORT NUMBER: SAMTEC TR-79-2	2. GOVT ACCESSION NO.
3. RECIPIENT'S CATALOG NUMBER	
4. TITLE *(and Subtitle)*: RANGE VERNIER	5. TYPE OF REPORT & PERIOD COVERED: FINAL REPORT. Jun thru Aug 1979
6. PERFORMING ORG. REPORT NUMBER: PA300-T-39-32	
7. AUTHOR(s): RUSSELL ROY	8. CONTRACT OR GRANT NUMBER(s): SPACE AND MISSILE TEST CENTER Contract No. F04703-77-C-0111
9. PERFORMING ORGANIZATION NAME AND ADDRESS: PERFORMANCE ANALYSIS DEPARTMENT FEDERAL ELECTRIC CORPORATION, WTR DIVISION	10. PROGRAM ELEMENT, PROJECT, TASK AREA & WORK UNIT NUMBERS: 78032F F04703-77-C-0111
11. CONTROLLING OFFICE NAME AND ADDRESS: SPACE AND MISSILE TEST CENTER (AFSC) CODE XRXM VANDENBERG AFB, CALIFORNIA 93437	12. REPORT DATE: 30 August 1979
	13. NUMBER OF PAGES: 43
14. MONITORING AGENCY NAME & ADDRESS *(if different from Controlling Office)*	15. SECURITY CLASS. *(of this report)*: Unclassified
	15a. DECLASSIFICATION/DOWNGRADING SCHEDULE

16. DISTRIBUTION STATEMENT *(of this Report)*

Approved for public release; distribution unlimited.

17. DISTRIBUTION STATEMENT *(of the abstract entered in Block 20, if different from Report)*

18. SUPPLEMENTARY NOTES

19. KEY WORDS *(Continue on reverse side if necessary and identify by block number)*

Precise Radar Ranges, Doppler Phase Extraction - Pulse Doppler Radars

20. ABSTRACT *(Continue on reverse side if necessary and identify by block number)*

A collection of technical information pertaining to Range Vernier implementation on Coherent Signal Processor (CSP) radars at the Western Test Range (WTR) is presented. The Range Vernier technique is quite recent, having evolved since mid 1976. Under certain operational conditions, the technique can provide radial range measurements with Root Mean Square (RMS) noise values at subwavelength levels, plus modelable systematic error components. Measurements of such quality can significantly improve WTR metric test support

DD FORM 1 JAN 73 1473 EDITION OF 1 NOV 65 IS OBSOLETE

UNCLASSIFIED

SECURITY CLASSIFICATION OF THIS PAGE *(When Data Entered)*

411 113

Cont'

capabilities.

The information includes descriptions of the technique, mathematical construction of range measurements, mechanization techniques and requirements, together with error models. Also, potential applications and feasibility testing are discussed.

SUMMARY

A collection of technical information pertaining to Range Vernier implementation on Coherent Signal Processor (CSP) radars at the Western Test Range (WTR) is presented. The Range Vernier technique is quite recent, having evolved since mid 1976. Under certain operational conditions, the technique can provide radial range measurements with Root Mean Square (RMS) noise values at sub-wavelength levels, plus modelable systematic error components. Measurements of such quality can significantly improve WTR metric test support capabilities.

The information includes descriptions of the technique, mathematical construction of range measurements, mechanization techniques and requirements, together with error models. Also, potential applications and feasibility testing are discussed.

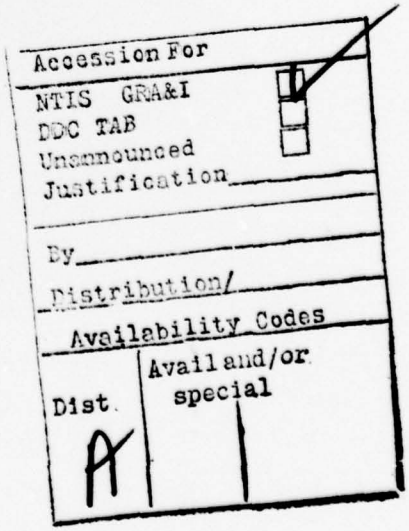

ACKNOWLEDGEMENT

The insight of Dr. R. A. Brooks regarding the potential value of Doppler phase information to subsequent derivation of very precise range measurements, together with his innovative creation of the basic Range Vernier formulations are gratefully recognized. Also, the content of his paper "Doppler Range Technique (Range Vernier)" has provided the principal source of information presented herein. Even more, the report that follows could not have been written without the results of Dr. Brooks efforts; so indeed, his contributions are sincerely appreciated.

TABLE OF CONTENTS

TABLE OF CONTENTS
(Continued)

LIST OF FIGURES

LIST OF TABLES

1.0 INTRODUCTION

Since mid 1976, the Space and Missile Test Center (SAMTEC) at Vandenberg Air Force Base has been investigating a technique called Range Vernier whereby radial range measurements are derived from the phase of signals that are received during operations of certain pulse Doppler radars on the Western Test Range (WTR). These radars, termed CSP radars, perform fine line tracking of Doppler frequencies. Implementation of Range Vernier involves extraction and recording of Doppler phase measurements, and subsequent conversion to radial range measurements. The latter measurements are called Doppler ranges.

The theoretical quality of extreme precision plus modelable error components to be provided by Doppler ranges, offers an opportunity to greatly improve accuracies of WTR tracking instrumentation. In addition to improving the quality of range data per se, the excellent precision of the range measurements is especially suited to substantial improvement of (a) trajectory reconstruction, (b) instrumentation performance analysis, (c) weapon system analysis, and in some cases, (d) refinement of geodetic, geopotential, and meteorological models. Each of those factors is fundamental to the principal measurement objectives of test mission support.

The purpose of this document is to support further SAMTEC development of Range Vernier capabilities by presenting technical information that is relevant to the technique in general, and that is directly pertinent to implementation of the technique on CSP radars at the WTR[1]. A major portion of the technical material presented herein has been collected from the documents cited in the References, page 34, especially the paper by Dr. R. A. Brooks, Reference [1].

The following sections include a background and conceptual definition of the Range Vernier technique, discussion of Doppler cycle ambiguity resolution, mechanization and requirements of Doppler phase measurements, analysis of Doppler range errors, various applications of Doppler ranges, a discussion of feasibility testing, and a summary.

---

[1] A SAMTEC task to implement a prototype Range Vernier subsystem on the FPQ-6 CSP radar at Pillar Point, California is currently in progress.

2.0 RANGE VERNIER CONCEPT

Fundamentals of a certain technique whereby Doppler frequency measurements are combined with small fractional measurements of Doppler phase angles to subsequently derive very precise measurements of radial ranges are described in this section. The technique, called "Range Vernier", is intended for application to data provided by a pulse Doppler tracking radar (i.e. a CSP radar) that is augmented with Doppler phase measurement capabilities.

2.1 Basic Relation

To establish a basic relation between the Doppler phase $\Theta_d(t)$ of a signal reply to the radar at time t and the range R from the radar to the object being tracked, consider a radar that is operating with a stable transmitter frequency f_o, and assume there is no time delay of this signal at the target. Consequently, the phase Θ_o of this coherent signal is varying according to the constant rate $2\pi f_o$, and the difference $\Theta_o(t_a) - \Theta_o(t_b)$ of this transmitter signal phase between times t_a and t_b is

$$\Theta_o(t_a) - \Theta_o(t_b) = 2\pi f_o[t_a - t_b] \quad . \tag{2.1}$$

Also, let R(t') be the range corresponding to t', and let τ' be the one-way transit time, so that the time t of signal reply at the radar is $t = t' + \tau'$. The Doppler phase $\Theta_d(t)$ of this signal reply is defined by the equation

$$\Theta_d(t) = \Theta_o(t) - \Theta_o(t - 2\tau') \quad .$$

Thus, because of equation (2.1),

$$\Theta_d(t) = 2\pi f_o[t - (t - 2\tau')] = 4\pi f_o \tau' \quad .$$

The preceeding relation is equivalent to the expression

$$\Theta_d(t) = \frac{4\pi}{\lambda} R(t') \quad , \tag{2.2}$$

where $\lambda = C/f_o$ is the wavelength; $R(t') = C\tau'$; and C is the speed of light through the medium.

In other words the range $R(t')$ at the retarded time t' is equal to the scalar $\lambda/4\pi$ times the Doppler phase of the signal reply at time t.

2.2 Range Measurement Construction

During operation, a pulse Doppler tracking radar provides a continuous reference signal with constant frequency f_o. The transmitted signal however, consists of a train of pulse modulated bursts of the reference signal. The bursts are separated in time according to some specific pulse repetition frequency f_r. Therefore, direct measurement of Doppler phase between pulses is not possible due to absence of signal replies between pulses. However, consideration of the true delta-phase D_i between successive pulses is practical; that is consideration of the difference

$$D_i = \theta_{i+1} - \theta_i$$

where

$$\theta_{i+1} = \theta_d(t_{i+1}) \quad \text{and} \quad \theta_i = \theta_d(t_i) \ .$$

A vital point of the Range Vernier technique is that the signal present during a pulse reply can be passed through a measurement subsystem (discussed in Section 4.0) to obtain certain angular measurements $\tilde{\theta}_i$. These are small fractions of the total Doppler phases θ_i. More specifically, each $\tilde{\theta}_i$ is a measurement of the true Doppler phase θ_i, modulo 2π plus an error ε_i. That is,

$$\tilde{\theta}_i = \theta_i - 2K_i\pi + \varepsilon_i \ , \qquad (2.3)$$

where K_i is a positive integer such that $0 \leq \theta_i - 2K_i\pi < 2\pi$ and ε_i is the error of $\tilde{\theta}_i$.

Notice that

$$\tilde{\theta}_{i+1} - \tilde{\theta}_i = D_i - 2N_i\pi + \varepsilon_{i+1} - \varepsilon_i \quad , \tag{2.4}$$

where

$$N_i = K_{i+1} - K_i \quad .$$

N_i is the count (or multiple) of complete Doppler phase cycles between successive pulse replies. The integer N_i can be determined with an ambiguity resolution technique described later in Section 3.0. Accordingly, the $\tilde{D}_i$ defined below is a measurement of D_i

$$\tilde{D}_i = \tilde{\theta}_{i+1} - \tilde{\theta}_i + 2N_i\pi \quad . \tag{2.5}$$

Also, using equation (2.4), an equivalent expression is

$$\tilde{D}_i = D_i + \varepsilon_{i+1} - \varepsilon_i \quad .$$

In order to continue construction of ranges, form the sum

$$\tilde{S}_n = \tilde{D}_o + \tilde{D}_1 + \cdots + \tilde{D}_{n-1}$$

of delta-phase measurements $\tilde{D}_i$, $0 \leq i \leq (n-1)$.

Straight forward calculation of the right hand side of $\tilde{S}_n$ shows that

$$\tilde{S}_n = \theta_n - \theta_o + \varepsilon_n - \varepsilon_o \quad .$$

A key point is that due to mutual cancellation, the Doppler phases θ_j and the errors ε_j for $0 < j < n$ vanish in calculation of the sum. This feature, zero accumulation of errors ε_j, is very important to precision of the range construction with the Range Vernier technique. To continue explanation of the range construction, the measurement $\Delta\tilde{R}_n$ is defined by the equality

$$\Delta\tilde{R}_n = \alpha\tilde{S}_n$$

where $\alpha = (\lambda/4\pi)$ and λ is the wavelength of the reference signal. Recall, from the basic relation of equation (2.2), that α is the scalar needed for conversion of Doppler phase angles to range units, therefore

$$\Delta\tilde{R}_n = R_n - R_o + \alpha\varepsilon_n - \alpha\varepsilon_o \quad .$$

A range ambiguity exists at this stage of construction due to the unknown value R_o; but, in practice, a measurement $\bar{R}_o$ of R_o can be obtained from the range subsystem of the radar (or from other measurement sources) such that $\bar{R}_o = R_o + E_o$, where E_o is the error of $\bar{R}_o$.

Accordingly, the calculation

$$\tilde{R}_n = \Delta\tilde{R}_N + \bar{R}_o$$

determines a range $\tilde{R}_n$ constructed with the Range Vernier technique. Ranges determined in this manner are called "Doppler ranges".

Additional calculations lead to the expression

$$\tilde{R}_n = R_n + B_o + \alpha\varepsilon_n \quad , \text{ where } \quad B_o = E_o - \alpha\varepsilon_o \quad .$$

This indicates that as n increases, the errors $(\tilde{R}_n - R_n)$ consist of two components, a constant bias term B_o and a time varying error $\alpha\varepsilon_n$. A more complete discussion of Doppler range errors is presented in Section 5.0.

Measurements from sources other than Doppler phase information are needed to determine the multiple N_i of complete Doppler phase cycles between successive pulse replies that is shown in equation (2.5) above. A technique that can be used to determine N_i, and consequently resolve Doppler phase ambiguity is described in the next section.

3.0 AMBIGUITY RESOLUTION

The construction of range measurements determined with the Range Vernier technique described above in Section 2.2, assumes that ambiguities of the delta-phase measurements have been resolved. These particular ambiguities are due to the unknown numbers N_i of complete cycles of the Doppler phase that occur between successive signal replies. This section herein describes a method to resolve delta-phase ambiguities by determination of the integers $\tilde{N}_i$ such that $\tilde{N}_i = N_i$.

A conceptual background and general conditions that are sufficient to resolution of delta-phase ambiguity are presented in Section 3.1.

A particular technique to resolve delta-phase ambiguity is described in Section 3.2. The technique combines Doppler phase measurements with conventional Doppler frequency measurements. Also, the technique assumes that ambiguities of the latter frequency measurements have been resolved.

In order to complete this discussion of ambiguity resolution, several methods that can provide unambiguous Doppler frequencies are mentioned in Section 3.3.

3.1 Ambiguity Background

The problem of ambiguity resolution can be addressed by consideration of the fundamental derivative expression that relates Doppler phase Θ_d to Doppler frequency, namely

$$\frac{1}{2\pi} \frac{d\,\Theta_d(t)}{dt} = F_d(t) \quad . \tag{3.1}$$

For the continuous case, (3.1) can be integrated to obtain the expression

$$D_i = \theta_d(t_{i+1}) - \theta_d(t_i) = 2\pi \int_{t_i}^{t_{i+1}} F_d(t)dt \ , \text{ where}$$

Where D_i is the delta-phase between t_i and t_{i+1}. The integral on the right hand side can be expressed as an integer N_i plus a non-negative fraction q_i that is less than 1 to obtain the expression

$$D_i = 2\pi (N_i + q_i) \ .$$

This shows that the number N_i of complete cycles of Doppler phase between times t_i and t_{i+1} can be determined by integration of the Doppler frequencies.

However, in contrast to the continuous case, operation of a CSP radar provides the Doppler frequency measurement $\tilde{F}_d(t_i)$ at discrete times t_i according to a specific pulse repetition frequency f_r. As a consequence, the integral of Doppler frequencies must be approximated between successive pulse replies that are separated by $1/f_r$ units of time; i.e., $t_{i+1} - t_i = 1/f_r$. Integral approximation is not difficult for customary test operations at the WTR because in test missions, Doppler frequencies vary slowly and very good approximations to the integral can be made, provided that ambiguities are not present in the measurements $\tilde{F}_d(t_i)$.

To continue this background discussion of the method described in Section 3.2 below, consider the following general case.

Assume the $\bar{D}_i$ is an estimate of D_i that has been previously determined, for instance by approximation of the Doppler frequency integral or from some arbitrary source. Also, let $\delta\bar{D}_i$ be the error of $\bar{D}_i$.

Let the delta-phase measurement $\tilde{D}_i$ be defined by

$$\tilde{D}_i = \tilde{\theta}_{i+1} - \tilde{\theta}_i + 2L_i\pi \ , \qquad (3.2)$$

where $\tilde{\theta}_{i+1}$ and $\tilde{\theta}_i$ have been obtained from a Doppler phase measurement subsystem and L_i is an integer such that

$$\left| \bar{D}_i - \tilde{D}_i \right| < \pi$$

For this measurement of $\tilde{D}_i$ and selection of L_i, a sufficient condition for correct resolution of the delta-phase ambiguity is the inequality

$$\left| \delta\bar{D}_i - (\varepsilon_{i+1} - \varepsilon_i) \right| < \pi \quad . \tag{3.3}$$

This condition is not difficult to meet in practice whenever Doppler frequencies have been resolved, because with operational CSP radars and $f_r = 160$ Hz, $\delta\bar{D}_i$ is less than 2.25 degrees and $(\varepsilon_{i+1} - \varepsilon_i)$ is less than 15 degrees.

For this example, $\left| \delta\bar{D}_i - (\varepsilon_{i+1} - \varepsilon_i) \right| < 17.25$ degrees. This would certainly satisfy the condition for resolution of the delta-phase ambiguity. The above background shows the need of a solution for the unknown value of the integer L_i. A procedure whereby L_i can be evaluated is described in the next subsection.

3.2 Delta-Phase Ambiguity Resolution

The ambiguities of Doppler frequency measurements $\tilde{F}_d(t_i)$ are assumed to have been correctly resolved in this subsection. With this assumption, the calculational procedure to resolve delta-phase ambiguities can be described as follows.

Integrate[1] the two most recent Doppler frequencies $\tilde{F}_d(t_i)$ and $\tilde{F}_d(t_{i+1})$ corresponding to successive pulse replies to obtain the integer $\bar{N}_i$ and fractional value $\bar{q}_i$ such that

---

[1] A trapezoidal rule will provide the integral approximation

$$\frac{\bar{D}_i}{2\pi} = \frac{\tilde{F}_d(t_i) + \tilde{F}_d(t_{i+1})}{2} \quad \frac{1}{f_r} \quad , \text{ where } t_{i+1} - t_i = 1/f_r \quad .$$

$$\frac{\bar{D}_i}{2\pi} = \int_{t_i}^{t_{i+1}} \tilde{F}_d(t)dt = \bar{N}_i + \bar{q}_i \text{ where } 0 \leq \bar{q}_i < 1 \quad .$$

Then determine the comparison value

$$C_i = \bar{q}_i - \frac{\tilde{d}_i}{2\pi}$$

where $\tilde{d}_i = \tilde{\theta}_{i+1} - \tilde{\theta}_i$ and the direct phase measurements $\tilde{\theta}_{i+1}$, $\tilde{\theta}_i$ are obtained from the (I/Q) subsystem.

Notice the range of C_i is between -1 and 2 since $|\tilde{d}_i| < 2\pi$ and $0 \leq \tilde{q}_i < 1$.

Select the appropriate value of ΔN_i according to the functional list and range of values C_i below

ΔN_i	
-1	$-1 < C_i < -1/2$
0	$-1/2 \leq C_i \leq 1/2$
1	$1/2 < C_i \leq 3/2$
2	$3/2 < C_i < 2$

Calculate $L_i = \bar{N}_i + \Delta N_i$, and

$$\tilde{D}_i = \tilde{d}_i + 2\tilde{N}_i\pi \quad , \text{ where } \tilde{N}_i = L_i \tag{3.4}$$

As a consequence of this procedure the following inequality is satisfied

$$\pi > |\bar{D}_i - \tilde{D}_i| = |2(\bar{N}_i - L_i)\pi + 2\pi\bar{q}_i - \tilde{d}|$$

A point of interest here is that delta-phase ambiguities can be resolved for successive time instants t_i, i = 0, 1, ..., N provided that the measurements $\tilde{D}_i$ of equation (3.4) can be evaluated and the inequality of (3.3) is satisfied. Subsequently, the Doppler ranges $\tilde{R}_n$ corresponding to retarded times t'_n, n = 1, 2, ..., N can be derived with the construction of Section 2.2. However, in practice, there may be periods of time when the data are not acceptable or unavailable for calculation of Doppler ranges; e.g. no signal replies, gross errors, lack of unambiguous Doppler frequencies, etc. Whenever this occurs, the Range Vernier technique must be reinitialized and started at a new time instant t_o^* that is followed by successive time instants that do provide acceptable data. This implies a new range measurement $\bar{R}_o(t_o^*)$ must be provided, and that another estimate of the bias B_o, of Section 2.,0 is anticipated.

Due to the vital role that unambiguous Doppler frequencies play in the resolution of delta-phase ambiguities, a brief discussion of Doppler frequency ambiguity is presented in the next section.

3.3 Doppler Frequency Ambiguity

Doppler frequency ambiguities are considered to be resolved whenever the magnitudes of Doppler frequency errors are less than half of the pulse repetition frequency. This condition can be attained with several methods discussed below.

One method is to compare (a) range measurements collected by a range tracking subsystem with (b) measurements of range derived by integration of range rates obtained from Doppler frequency measurements collected by the Doppler tracking subsystem. The comparisons can be processed with a linear estimator, such as a Kalman type recursive filter or a batch least squares filter, to resolve Doppler frequency ambiguitites. A particular example of this method is described in the Appendix.

Another method involves use of an Invariant Embedding technique to resolve frequency ambiguities. This method is currently available with CSP radars. It is described in Reference [2].

Either of the two above methods is feasible for realtime or post-flight data reduction purpose. However, a comparison of the methods indicates that the former is suitable for more rapid ambiguity resolution than the latter. Rapid ambiguity resolution is crucial to realtime applications, so the former method is a strong candidate for future implementation.

A third method is to transform coordinates of a suitably accurate estimate of the trajectory to measurements of Doppler frequencies that are unambiguous. More generally, this can be done in post-flight applications, when an accurate best estimate of trajectory (BET) is available.

Accordingly, there are several methods whereby Doppler frequency ambiguities can be resolved as required by the delta-phase ambiguity resolution that is described in Section 3.2.

4.0 MECHANIZATION

Mechanization of Doppler phase measurements at Coherent Signal Processor (CSP) Radars of the Western Test Range (WTR) is discussed in this section. Essentially, extraction and recording of Doppler phase and frequency is involved.

4.1 Background Discussion

A block diagram of a SAMTEC Doppler radar (CSP radar of interest) displaying the signals and nominal frequencies at various system modes, is illustrated in Figure 4.1. The stable clock and the frequency synthesizer are external to the tracking loop, but provide the reference signals required for tracking loop operation as well as the transmitter carrier signal $e^{i\omega_o t}$.

The pulse amplitude modulated received signal arrives within the range gate window, and its carrier $e^{i[\omega_o t-\Theta]}$ contains the Doppler phase modulation Θ. Internal to the tracking loop, a digital frequency synthesizer (DFS) develops a signal $e^{i[\omega_L t-\Theta']}$ with phase modulation Θ' approximately equal, modulo 2π, to the Doppler phase Θ. This signal is translated in frequency and heterodyned with the received signal to obtain the IF input signal. The IF bandwidth is approximately matched to the received pulsewidth, and consequently the SNR at the IF output is near optimum. The IF output signal carrier is $e^{i[\omega_I t+\Delta\Theta]}$, where $\Delta\Theta = \Theta - \Theta'$, and thus this signal together with the digital frequency synthesizer signal $e^{i[\omega_L t-\Theta']}$ jointly contain the Doppler phase information.

The conventional Doppler frequency output is shown as $\tilde{F}_d$, but the remainder of the tracking loop signals and operations are not germane to the current discussion and will not be considered further.

4.2 Doppler Phase Measurement

Doppler phase measurement could be accomplished at the input of the Doppler tracker by direct comparison of the phases of the received signal and transmitter carrier, but there are several reasons why this technique may not be preferred.

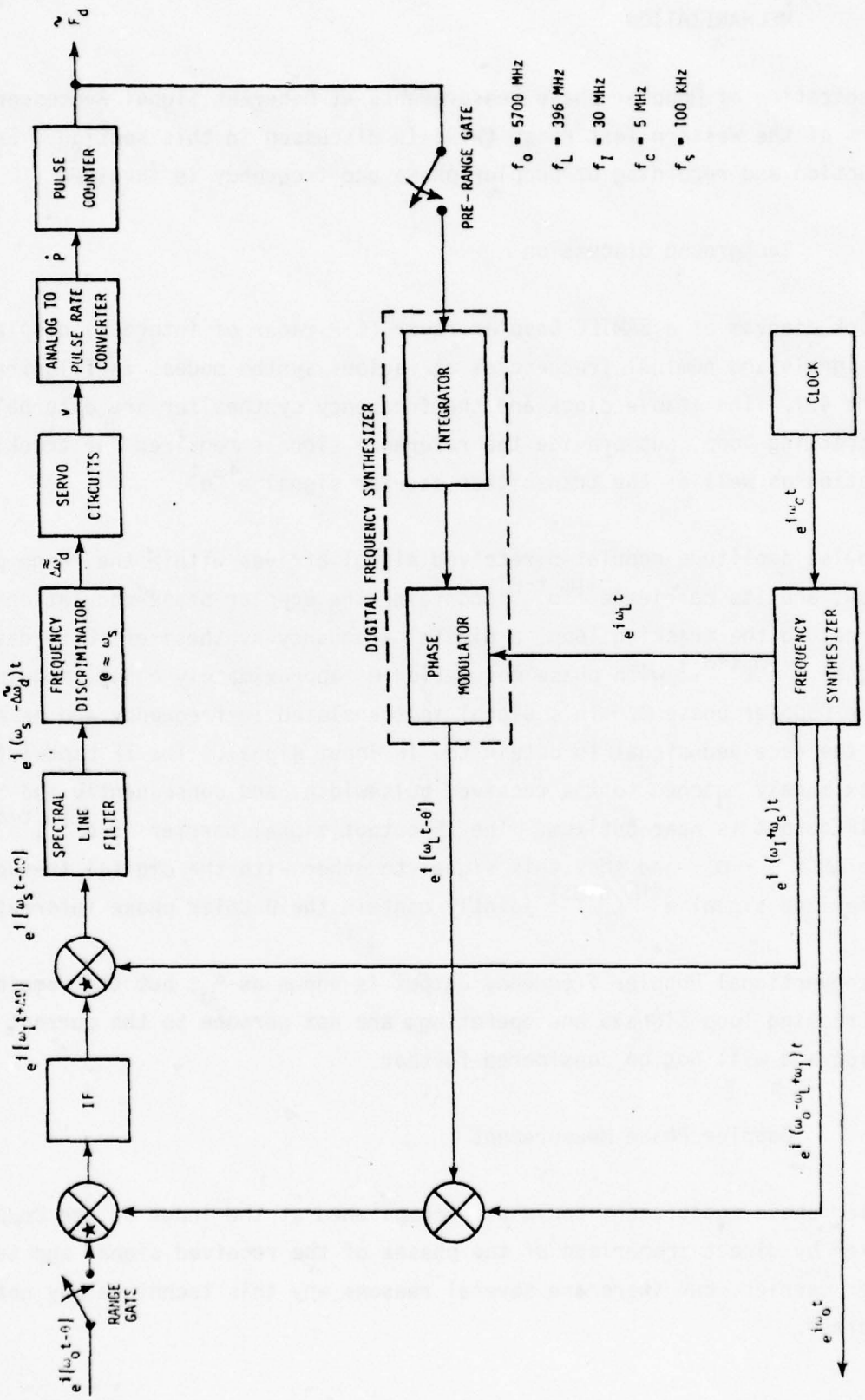

FIGURE 4.1 SAMTEC DOPPLER TRACKER

First, in order to enhance the SNR, it is necessary to filter the received signal prior to measuring its phase. For near optimum SNR, the filter bandwidth should be matched to the received pulsewidth. But the filter bandwidth must also be large enough to accommodate the band of Doppler frequencies, and moreover, unless the bandwidth greatly exceeds this band, the filter will introduce phase error in amounts related to the instantaneous Doppler frequency. Thus, some compromise in SNR may result from a filter designed to have a constant phase response over the Doppler frequency band.

Second, when the Doppler frequency is of sufficient magnitude to produce a substantial change in the Doppler phase within the received pulse, precise timing of the phase measurement is required. Thus direct comparison of the received signal and transmitter carrier phases requires measurement at a precisely timed point within the received pulse. This can be accomplished with high speed circuitry, but since only a portion of the received pulse is used, some information is lost and measurement performance is degraded. It is also possible to compute the average phase over the entire pulse, but then uncertainty in the time tag to be applied to the measurement is created by intrapulse amplitude fluctuations as well as pulse time of arrival error induced by noise.

Third, in systems which employ pulse coding, it is necessary to pass the received pulse through a matched filter prior to extracting the Doppler phase. The performance of the matched filter may be enhanced by, or in some cases critically dependent upon, Doppler frequency and time dilation compensation. This compensation requires closed loop operation which is not consistent with the direct measurement of Doppler phase by simply comparing the phases of the received signal and transmitter carrier.

An indirect method of Doppler phase measurement is conceptually illustrated in Figure 4.2. In the upper channel the phase of each received pulse is measured at the IF output, and in the lower channel the phase of the DFS output signal is also measured. The phase measurements in these two channels are then summed to obtain the Doppler phase measurement.

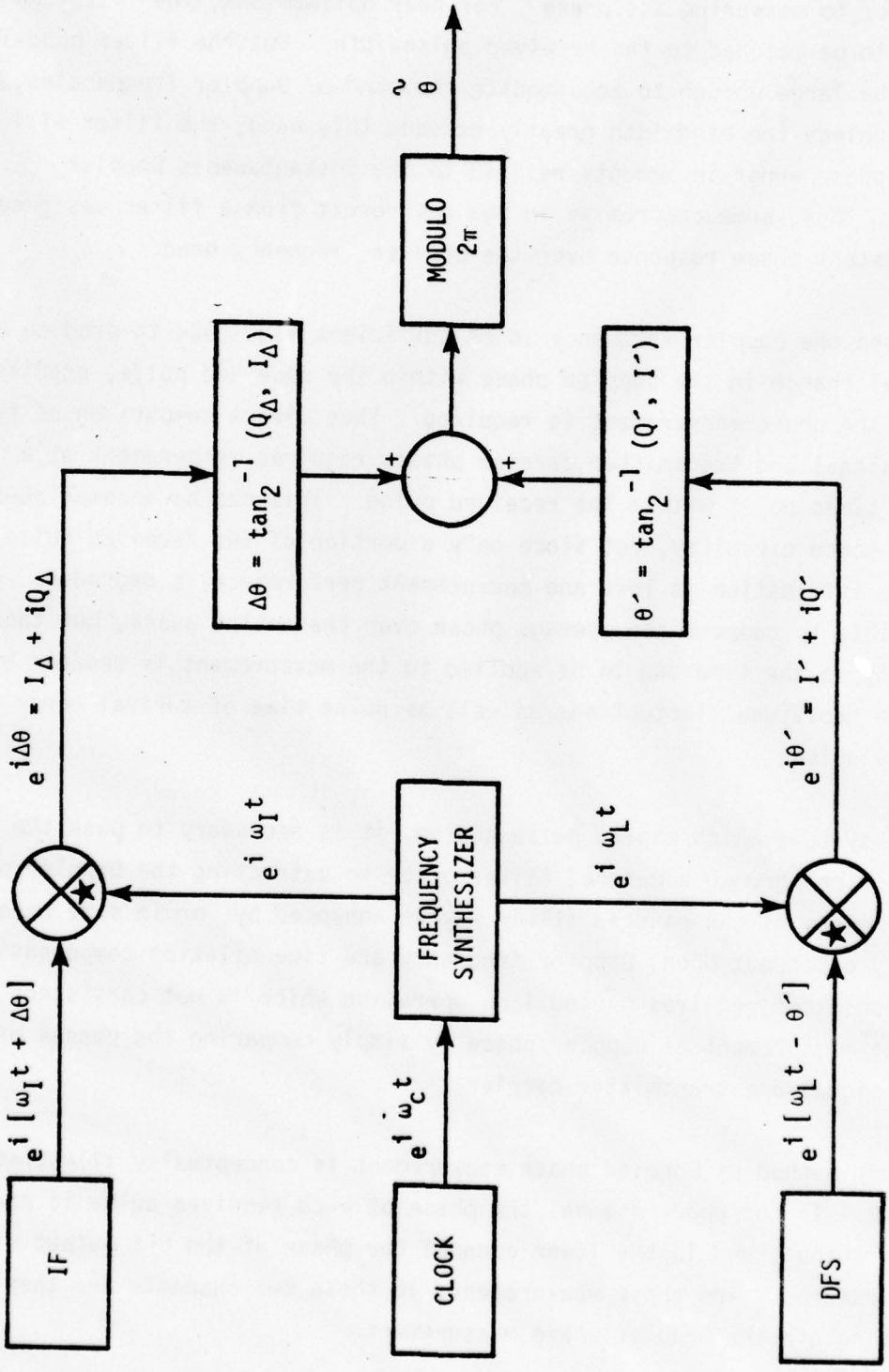

FIGURE 4.2 DOPPLER PHASE MEASUREMENT

When the system is tracking properly, the phase variation within each pulse in the upper channel is negligible. Thus the average phase over the pulse is measured, and precise timing of the measurement is unnecessary. On the other hand, the phase of the DFS signal is varying at a rate approximately equal to instantaneous Doppler angular frequency, and precise timing of the phase measurement in the lower channel is required. However, the DFS output signal is continuous and noisefree, and consequently precise measurements of phase and time at any point for this signal can be obtained with readily available hardware components. It is important to note that, although the time of the phase measurement must be precisely measured, the actual time at which the phase measurement occurs is not too critical; generally it suffices for the measurement time to be anywhere within or very near the range gate.

A specific mechanization for the indirect method of Doppler phase measurement is illustrated in Figure 4.3, and two options are presented for the measurement of the DFS output signal.

The IF output signal is passed through a saturating amplifier and harmonic rejection filter prior to phase measurement in order to normalize the signal level at the input of the I/Q device. The bandwidths of the amplifier and filter must be greater than the IF bandwidth in order to not distort the IF phase information. However, the harmonic rejection filter should provide at least 40 dB attenuation of all IF harmonics in order to ensure negligible mechanization error. The I/Q ouputs are averaged over the range gate window to obtain I_{Δ} and Q_{Δ}.

In the first option for DFS output processing, a simple I/Q device is used, and its outputs are sampled at precise times which can be controlled by a clock driven trigger within the range gate.

In the second option, a commercially available computing counter is used to precisely measure the time interval between positive slope zero crossings of the clock signal and the DFS output signal (after translation to the clock frequency). The arming signal is generated by a negative slope zero crossing

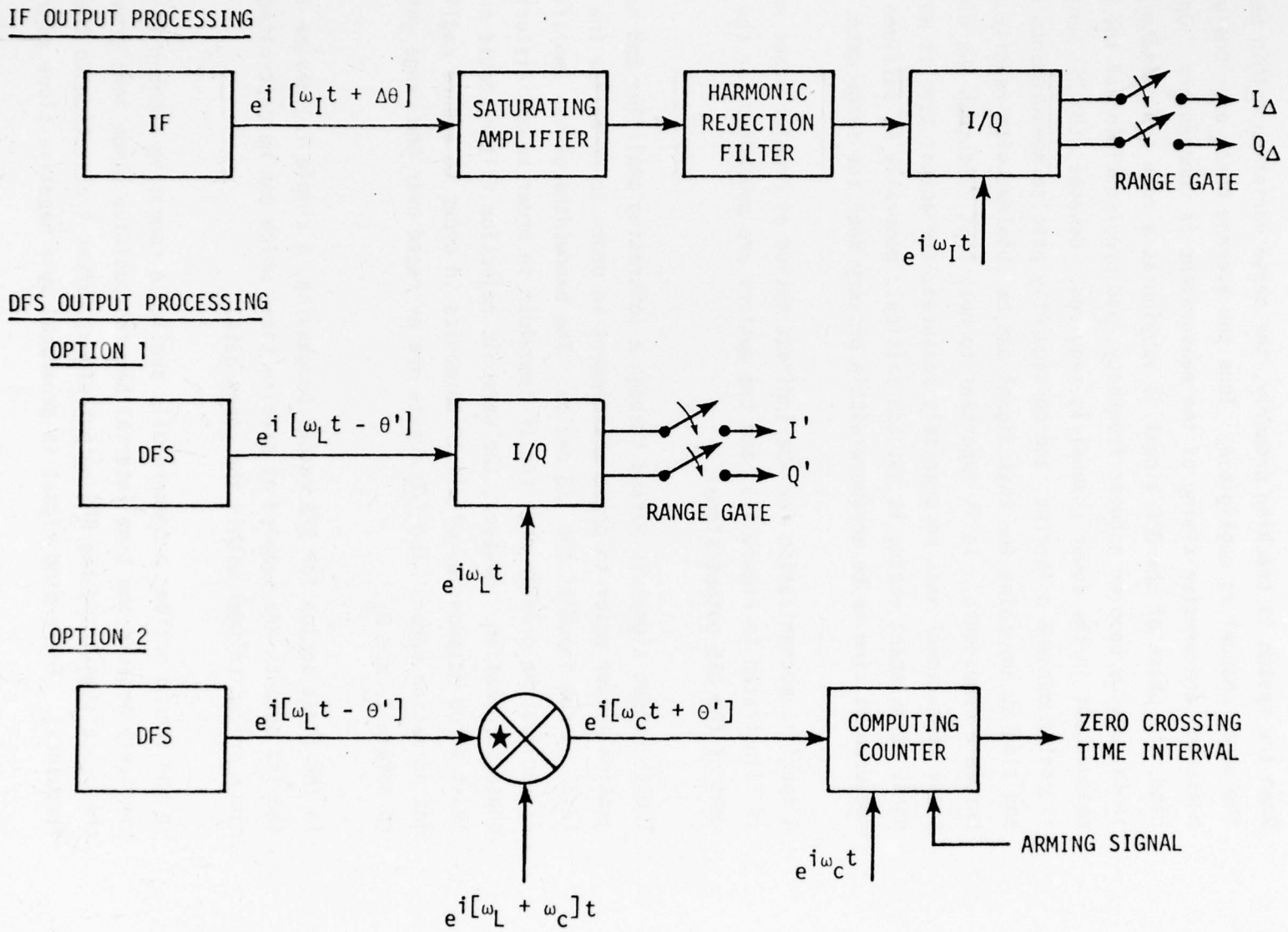

FIGURE 4.3 MECHANIZATION OF DOPPLER PHASE MEASUREMENT

of the clock signal selected to be within the range gate. Thus the time t_- of the arming signal is known, and the computing counter measures the time interval (with proper sign) between the first positive slope zero crossing to follow arming. Using the known time of the arming command t_- and the measured time interval TI, it follows that $\theta' = -\omega_c(TI)$ at

$$\tilde{t} = t_- + \frac{\pi}{\omega_c} + TI \quad ,$$

and thus the measured Doppler phase at time $\tilde{t}$ is simply

$$\tilde{\theta}(\tilde{t}) = \Delta\theta - \omega_c(TI).$$

The rms timing precision achievable by this technique is better than 0.1 nanosecond.

4.3 Mechanization Requirement

A listing of mechanization requirements pertinent to implementation of the I/Q measurement sub-system is presented in Table 4.1. Also, a historical record of the Doppler frequency measurements corresponding to successive replies at times t_i, t_{i+1}, ... is required. These frequencies should be recorded at the pulse repetition rate, i.e. f_r per second.

TABLE 4.1 MECHANIZATION REQUIREMENTS

RECORDING RATE	I', Q' (OR θ') PRF	I_Δ, Q_Δ (OR $\Delta\theta$) PRF
SYNCHRONIZATION	COINCIDENT WITH RANGE GATE TO NEAREST 1 μSEC	COINCIDENT WITH RANGE GATE
TIME TAG LSB JITTER (1 σ)	1 μSEC $\leq$ 0.05 μSEC	N/A
QUANTIZATION WORD LENGTH*	8 BITS	8 BITS
SYSTEM MECHANIZATION ERROR	$\leq 1.5°$	$\leq 1.5°$

* FULL WORD REPRESENTS EITHER 360° IN θ OR 1 IN I, Q.

5.0 ERROR ANALYSIS

A general model of the error present in range measurements determined with the Range Vernier technique was mentioned in Section 2.2. The general model is expanded herein to recognize more components of the basic error sources.

5.1 Range Vernier Error Model

The expanded error model is

$$\tilde{R}_i = R_i + \delta B + (\dot{R}_i - \dot{R}_o)\delta t + (R_i - R_o)\delta F + \delta\rho_i - \delta\rho_o + \delta U_i - \delta U_o + v_i, \; i<0 \quad ,$$

where

- δB - bias due to initialization
- δt - systematic time tag delay error
- δF - scale factor error due to uncertainties in the speed of light and long term clock frequency
- $\delta\rho$ - refraction error
- δU - structurally unspecified errors due to transmitter/receiver mechanization, vehicle transponder/antenna/plume and scintillation
- v - serially uncorrelated phase measurement error due to noise, jitter, and quantization.

The first observation to be made is that the Doppler range measurement is subject to group delay and phase refraction. Thus the time at which the measurement applies, that is the retarded measurement time, is equal to the time of reception minus one-way group delay, or simply the time midway between pulse transmission and pulse reception (at the antenna). And the refraction term, which is with respect to the target position at the retarded measurement time, represents phase, rather than group, refraction at this position.

The bias error consists of the combined instantaneous values of the range tracker output error and the serially uncorrelated component of phase measurement error at initialization.

The timing error has components due to clock lag, differences in transmitter and receiver group delays, and sampler delay. Combining all terms, the systematic timing error has the form

$$\delta t = \delta t_C + \frac{\Delta T_T - \delta t_R + \delta t_S}{2} ,$$

where δt denotes uncompensated timing error, and the subscripts denote clock lag (C), receiver delay (R), transmitter delay (T), and sampler delay (S).

The scale factor error consists of a term due to the speed of light uncertainty (approximately 10^{-9}) and a term due to long term clock frequency uncertainty (approximately $5x20^{-11}$ for a cesium clock).

The serially uncorrelated phase errors are due to the receiver, clock, transponder, and sampler. Ignoring transponder phase noise, a typical worst case phase error budget for noise, jitter, and quantization in CSP radars is presented in Table 5.1. The Root Sum Squares (RSS) error is 6.2°, which is equivalent to an error in range of approximately 0.5 millimeter for f_o = 5 Gigahertz.

5.2 Transponder And Antenna Consideration

The coherent transponder and antenna equipment located on the vehicle of interest are vital subsystems of CSP radar tracking operations. Unsatisfactory performance of either subsystem can result in erroneous Doppler phase or frequency of the signal replies to the radar.

Insofar as the transponder is concerned, transponders under procurement for Minuteman III launches from WTR are required by contractual specification to remain frequency coherent within 0.6 Hertz smoothed over 0.1 second, but not required to be phase stable. Transponder tests being conducted at SAMTEC show phase stability within 0.001 Hertz under some environmental conditions, but also display phase variation due to signal strength, temperature, interogation rate and frequency, and vibration. Details of the test methodology and results will be reported on completion of the tests.

TABLE 5.1 RECEIVER RANDOM ERROR BUDGET

RECEIVER NOISE AT SNR = 20 dB

4.05°

CLOCK PHASE NOISE

0.12° (INTRA-PULSE)

2.1° (TRANSIT TIME: R = 5000 nmi)

TIMING JITTER (σ_t = 0.1 μsec)

4.1° ($\dot{R}$ = 20,000 ft/sec)

QUANTIZATION (8 BIT I/Q WORDS)

0.82°

RSS OF ABOVE ERRORS = 6.2°

A basic factor in the satisfactory performance of the transponder antenna is the stability of the phase delay with respect to changes in the aspect angle viewed from the radar, since this aspect angle will change as the missile moves along its flight path in addition to roll and pitch maneuvers. An ideal antenna would be the theoretical isotropic radiator located at the center of gravity of the vehicle, since it would produce no change in phase with aspect angle variation. The "worst case" would be two discrete radiating elements mounted diametrically opposite on the missiles' cylindrical surface wth equal power applied to each radiator. If the radiators were about 8 feet apart and the roll aspect angle was midway between the two radiators, a 1.26° change in roll aspect could result in 180° of Doppler phase change and signal strength nulls as deep as -20 dB. The Range Vernier system will interpret this change in phase as an erroneous change in range and the CSP system will interpret the phase change rate as an erroneous velocity change.

The closest approximation of the performance of the isotropic antenna commercially available appears to be the segmented micro strip antenna design. This design ideally will exhibit no change in phase with roll aspect angle, and 90° phase change with a 90° change in pitch aspect. It should be remembered that the antenna is a reciprocal device and any phase change induced in the received signal by the antenna will have added a like phase change when the reply is transmitted.

The purpose of this subsection is to emphasize that satisfactory performance of both the transponder and antenna subsystems is necessary to obtain the high potential accuracy achievable with the Range Vernier system.

6.0 RANGE VERNIER APPLICATIONS

Doppler ranges determined with the Range Vernier technique can provide very precise (or low noise) measurements of ranges. Very precise range measurements can substantially improve observability of trends, refinement of error models, and accuracy of the estimation process. In turn, this can significantly improve WTR support of weapon system test objectives. Particular examples that show substantial improvements gained from application of very precise ranges are presented in Sections 6.1 and 6.2 that follow.

Section 6.1 shows certain results that have been obtained by the XONICS Corporation with a technique called Phase-Derived-Range (PDR). Additional results and a description of PDR are presented in Reference [3]. The PDR technique can be viewed as a modified version of the Range Vernier concept that has been adapted for applications to skin tracking, in contrast to tracking a coherent transponder with a CSP radar. In view of the similarity of PDR and Range Vernier techniques, the results shown in Section 6.1 are indicative of contributions to data processing objectives that can be anticipated with Range Vernier.

A summary review of several established estimation techniques and the consequences of using Range Vernier type ranges with these techniques, relevant to the basic objectives of test mission support, is presented in Reference [1]. This reference also includes an example of Range Vernier contributions to Guidance Analysis that is presented in Section 6.2.

6.1 Operational Results

The operational results described herein were presented by XONICS, Inc. in the paper cited in Reference [3]. The results were obtained with the PDR technique mentioned above.

In lieu of operational results for the Range Vernier that is being developed at SAMTEC, and because of the similarity of the two techniques, it seems appropriate that a preview of results to be anticipated from future applications of Range Vernier can be gained from PDR results. Accordingly, one of several

case results presented in Reference [3] is repeated in Figure 6.1 that follows; other results are shown in the Reference but not repeated herein. The differences ΔR shown graphically in Figure 6.1 are comparisons of ranges from particular radars with a Best Estimate of the ballistic trajectory, from about 700,000 feet altitude to about 0.30 second before impact. Comparisons of ΔR obtained with PDR versus usual range measurements collected from three radars, can be made from the Figure. The radars were operating at VHF, S-Band, and C-Band frequency levels respectively. In all cases, PDR is decidedly superior and improved observability is attained.

An important quotation from the Summary of Reference [3] is

> "... . The improved precision of PDR when applied to trajectory analysis results in (1) improved pierce points, (2) observation of altitude variations, (3) improved ability to estimate high altitude drag and/or atmospheric density, (4) improved observation of ionospheric refraction effects, and (5) observation of signatures related to RV configuration which have diagnostic as well as discrimination applications. ..."

In other words, the theoretical implication that extremely precise range measurements will improve observability of parameters of interest to test missions, has indeed been confirmed with operational results. Moreover, increased observability gained with such range precision can facilitate identification, analysis, and evaluation of parameters and measurements that support test mission objectives.

6.2 Application To Guidance Analysis

One of the more difficult problems in ballistic missile flight testing has been the analysis of guidance system errors at the component level. Theoretical investigations into this problem have been conducted by several organizations [4], [5]. One measure of effectiveness which has been devised is the recovery ratio, defined as the square root of the ratio of a posteriori to a priori error variance. Thus for a given parameter, a lower recovery ratio implies more observability and better recovery through the estimation procedure.

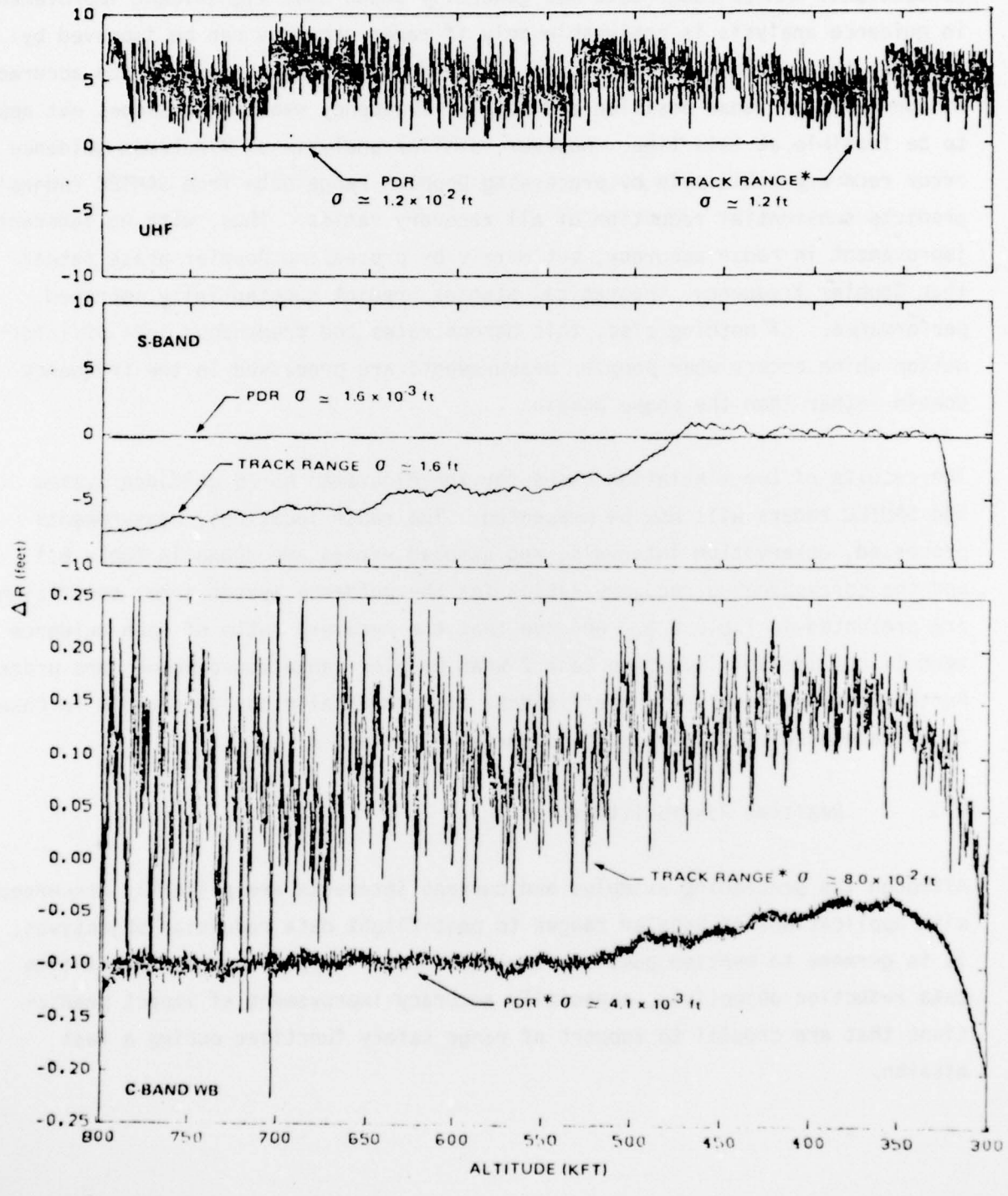

* Range history biased (for purposes of this illustration) to facilitate visibility

FIGURE 6.1 UHF, S-BAND AND C-BAND PDR AND TRACK RANGE VERSUS BALLISTIC BET

Analysis of Minuteman guidance error recovery ratios achievable by processing conventional SAMTEC radar data has generally shown that significant improvement in guidance analysis is achievable only if radar accuracy can be improved by some one to two orders of magnitude. Such dramatic improvement in the accuracy of conventional radar position and Doppler frequency measurements does not appear to be feasible at this time. However, similar analysis of Minuteman guidance error recovery achievable by processing Doppler range data from SAMTEC radars predicts substantial reduction of all recovery ratios. Thus, with no inherent improvement in radar accuracy, but merely by processing Doppler phase rather than Doppler frequency, theoretical studies predict substantially improved performance. If nothing else, this demonstrates the tremendous loss of information which occurs when Doppler measurements are processed in the frequency domain rather than the phase domain.

The results of two simulation cases for the Minuteman NS-20 guidance system and SAMTEC radars will now be presented. The radar locations, measurements processed, observation intervals, and assumed errors are shown in Table 6.1. and the corresponding recovery ratios for the guidance system error coefficients are presented in Table 6.2. Observe that the recovery ratio of each guidance term is considerably lower in Case 2 when Doppler range measurements are processed. Furthermore, although some coefficients are practically non-observable in Case 1, all are predicted to be quite observable in Case 2.

6.3 Realtime Possibilities

Although the preceeding examples and current interests are primarily concerned with applications of Doppler ranges to post-flight data reduction objectives, it is germane to mention possible applications of Doppler ranges to realtime data reduction objectives, especially accuracy improvement of impact predictions that are crucial to support of range safety functions during a test mission.

TABLE 6.1 RADAR SCHEDULE

	CASE 1					
RADAR CLASS	FPS-16	FPS-16	TPQ-18	FPQ-6	FPS-16	FPS-16
LOCATION	PT MUGU	SAN NICHOLAS ISLAND	VAFB	PILLAR PT	VAFB	PILLAR PT
MEASUREMENT TYPES	R,A,E,$\dot{R}$	R,A,E,$\dot{R}$	R,A,E,$\dot{R}$	R,A,E,$\dot{R}$	R,A,E	R,A,E
TRACKING INTERVAL TALO (SECONDS)	35-500	40-500	70-500	51-500	16-500	125-500
STANDARD DEVIATION						
BIAS	σ_R = 80 FT, σ_A = 0.15 MRAD, σ_E = 0.15 MRAD, $\sigma_{\dot{R}}$ = 0.5 FT/SEC					
NOISE	σ_R = 6 FT, σ_A = 0.15 MRAD, σ_E = 0.15 MRAD, $\sigma_{\dot{R}}$ = 0.1 FT/SEC					

	CASE 2			
RADAR CLASS	FPS-16	FPS-16	TPQ-18	FPQ-6
LOCATION	PT MUGU	SAN NICHOLAS ISLAND	VAFB	PILLAR PT
MEASUREMENT TYPE	R	R	R	R
TRACKING INTERVAL TALO (SECONDS)	35-500	40-500	70-500	51-500
STANDARD DEVIATION				
BIAS	σR = 80 FT			
NOISE	σR = 0.01 FT			

TABLE 6.2 GUIDANCE ANALYSIS RECOVERY RATIOS

GUIDANCE SYSTEM PARAMETER	RECOVERY RATIOS	
	CASE 1	CASE 2
PLATFORM MISALIGNMENT	0.7250 0.3143 0.5075	0.0065 0.0040 0.0152
GYRO BIAS (DRIFT RATE)	0.9887 0.8873 0.9437	0.0303 0.0568 0.0927
G-DEPENDENT DYRO BIAS	0.7896 0.7132 0.8127	0.0110 0.0382 0.0470
G^2-GEPENDENT DYRO BIAS	0.9041 0.5534 0.4799	0.0087 0.0087 0.0091
ACCELEROMETER BIAS	0.2369 0.3029 0.2637	0.0005 0.0009 0.0008
ACCELEROMETER SCALE FACTOR	0.4892 0.5308 0.5514	0.0013 0.0073 0.0075

Whenever systematic error terms of Doppler ranges have been verified, it will be possible to remove these error terms and provide corrected Doppler ranges. In turn, very accurate range rate measurements could be derived from polynominal smoothing of the corrected range data. This highly accurate range and range rate data could then be used to substantially improve the accuracies of estimated trajectories and subsequent estimates of predicted impact positions. Since it is feasible to consider performing these calculations during realtime data reduction, future considerations of possible applications of Range Vernier to realtime objectives is of practical importance to WTR test support.

7.0 FEASIBILITY TESTING

Implementation and operational testing of prototype Range Vernier systems are a major part of the development process, much knowledge will be gained as the tests evolve. Accordingly, a brief discussion of feasibility testing is presented herein.

Relevant to the ultimate goal of providing very precise Doppler range measurements with modelable systematic error terms, the essential objectives of feasibility testing are to

(1) demonstrate the operational ability of a CSP radar that is augmented with an (I/Q) measurement subsystem to provide the measurements required (Section 4.3) by the Range Vernier technique, and

(2) evaluate the ability to satisfactorily model the systematic and random components of errors that are present in the Doppler range measurements obtained from the tests.

Test data will be collected by tracking objects of opportunity. Analyses of the test data will be made to assess performance of the augmented system and to evaluate various components of the total Doppler range error. The total error will be determined by comparisons of the Doppler ranges with a best estimate of trajectory (BET) of the object that is tracked. Accuracy of the reference BET is crucial to evaluation of the total errors and subsequent evaluation of systematic and random (or "noise") error components. However, initial estimates of the noise component can be determined by smoothing the Doppler ranges with a low order polynomial, or by comparing the ranges with a smooth (not necessarily a "best") estimate of the trajectory.

Experience at SAMTEC has shown that a near earth satellite equipped with a coherent transponder antenna configuration for Doppler tracking, such as GEOS-C, is a practical object of opportunity for various tests. The GEOS-C satellite

offers (a) signal-to-noise levels sufficient to the needs of a CSP radar, (b) a smooth orbit that is amenable to determination of an accurate BET, (c) a cross-section that permits skin-tracking, and (d) the opportunity to schedule tests whereby sufficient time can be allocated for set-up and/or calibration of the radar immediately prior to actual tracking of the object.

Ballistic missiles such as Minuteman III, also provide objects of opportunity for feasibility tests. These tests are important since they will reflect the actual environment of a class of tests for which a completed Range Vernier system is intended to support. However, compared to satellite objects, several comments regarding Minuteman III objects are worthy of note; namely (1) repeated tests of the same airborne transponder/antenna configuration are impossible, (2) the latter configuration is not as stable as that of GEOS-C, and (3) generally speaking, the BET of a GEOS-C satellite can be more accurate than a BET of the more dynamic Minuteman vehicle. Regardless, of these comments, both GEOS-C type satellites and ballistic missile vehicles provide good objects of opportunity for feasibility testing.

A note of practical interest is that only a relatively modest augmentation of the data collection (radar) and data reduction (software) capabilities at SAMTEC is needed to conduct feasibility testing. This is because implementation of Range Vernier will make full use of current CSP radar capabilities - augmented with an (I/Q) measurement subsystem and recording equipment. Also, the analysis efforts will make full use of extensive computer programs that are currently available at SAMTEC. Only a relatively small computer program to convert the additional recorded data to Doppler range measurements is required to complete software capabilities needed for analysis of the feasibility test data.

8.0 SUMMARY

The Range Vernier technique is conceptually straight forward, and can be implemented by augmenting existing CSP radars with Doppler phase extraction and recording equipment. Alternative mechanization techniques and requirements for such equipment are presented. Development of a prototype Range Vernier system is in progress at SAMTEC, so a discussion of feasibility testing is included.

Resolution of Doppler ambiguities involved in Range Vernier and subsequent determination of Doppler ranges obtained with the technique are described. A linear model of systematic and random error components of Doppler ranges is provided, including consideration of error sources from an airborne transponder/antenna subsystem of a CSP radar.

Substantial improvements to test mission support obtained from application of very precise range measurements are demonstrated with operational and theoretical examples. The operational examples clearly show that improved observability, error recovery, and measurement accuracy have been achieved. The theoretical example indicates how precise range measurements can also facillitate guidance system analysis. Applications of operational Doppler ranges are anticipated to provide very precise range measurements and the improvements outlined above.

In addition to the post mission applications mentioned above possible application of Doppler ranges to realtime data reduction performed for range safety is discussed.

REFERENCES

1. Brooks, Richard A., "Doppler Range Technique (RANGE VERNIER)", paper presented at the Symposium On Moving Target Diagnostics Using Radar Data, held at the Mitre Corporation, McLean, Virginia, 19 April 1979.

2. "Radar Set AN/FPQ-6 Coherent Signal Processor Modification" prepared under contract F04701-71-C-0228, RCA Government and Commercial Systems Missile and Surface Radar Division, Moorestown, New Jersey.

3. Fletcher, E. T. and Young, N. A., "Phase-Derived-Range Technique And Recent Applications", paper presented at the Symposium on Moving Target Diagnositics Using Radar Data, held at the Mitre Corporation, McLean, Virginia, 19 April 1979.

4. Hertzog, R. T., et al, "Advanced Metric System Final Report," (U), TRW Corporation, 26948-6009-TE-01, for the Space and Missile Test Center, Vandenberg AFB, California, September 1975. SECRET.

5. Hopkins, M., "Guidance Diagnostics/Guidance Hardware Total Accuracy Support Capability On The Western Test Range", Technical Report Number PA-100-77-17, Space and Missile Test Center, Vandenberg AFB, California, April 1977.

6. Pickett, R. B., "Ambiguous Range Study Report", Technical Report Number PA100-77-18, Space and Missile Test Center, Vandenberg AFB, California, June 1977.

APPENDIX

An example of a method whereby Doppler frequency ambiguities can be rapidly resolved is described herein. The method, previously mentioned in Section 3.3, processes delta-ranges from two sources with a linear estimator to establish ambiguity resolution. The sources are (a) Doppler frequencies of the fineline tracking loop and (b) ranges from the range tracking subsystem of a CSP radar. The linear estimator can be a batch least squares, or a recursive Kalman type estimator. The former estimator is used in the example described below. In either case, the method is a feasible candidate for realtime or post-mission resolution of Doppler frequency ambiguities.

To begin discussion, let t_i ($i = 0, 1, \ldots, N$) be an increasing sequence of time instants corresponding to Doppler frequency measurements $\tilde{F}_i$ of successive signal replies at the radar and assume that a single fineline of the pulse frequency spectrum is being tracked from t_i through t_N. The error $\delta\tilde{F}_i$ of $\tilde{F}_i$ consists of a small random component $\tilde{\varepsilon}_i$ and an unknown multiple ΔN of the pulse repetition frequency f_r. More specifically,

$$\delta\tilde{F}_i = (\tilde{F}_i - F_i) = \Delta N f_r + \tilde{\varepsilon}_i \quad , \tag{A.1}$$

where ΔN is zero, a positive, or a negative interger, F_i is the true Doppler frequency, and the errors $\tilde{\varepsilon}_i$ are serially uncorrelated, with zero mean and variance $\tilde{\sigma}^2$.

Since F_i is related to the range rate $\dot{R}(t_i')$ corresponding to the retarded time t_i' by the equality

$$F_i = \frac{2\dot{R}(t_i')}{\lambda[1 + \dot{R}(t_i')/C]}$$

where C is the speed of light and λ is the wavelength of the reference frequency, integration provides the delta-range measurement $\Delta\tilde{R}_n$

$$\Delta\tilde{R}_n = \frac{\lambda}{2} \int_{t_o}^{t_n} \tilde{F}_i(t)dt \ , \qquad n = (1, 2, \ldots, N),$$

where the small term $\dot{R}(t_i')/C$ has been omitted for simplicity of exposition. Accordingly, $\Delta\tilde{R}_n$ is a measurement of the true delta-range $\Delta R_n = (R_n - R_o)$ plus an error $\delta\tilde{R}_n$.

The error can be determined by integration of (A.1) above, that is,

$$\delta\tilde{R}_n = \frac{\lambda}{2} \int_{t_o}^{t_n} \Delta N f_r dt + \frac{\lambda}{2} \int_{t_o}^{t_n} \tilde{\varepsilon}_i dt$$

Consequently,

$$\delta\tilde{R}_n = \frac{\lambda}{2} f_r(t_n - t_o)\Delta N + \tilde{\varepsilon}(n) \ ,$$

where $$\tilde{\varepsilon}(n) = \frac{\lambda}{2} \int_{t_o}^{t_n} \tilde{\varepsilon}_i dt \ .$$

To continue discussion, let R_n and $\bar{R}_o$ be ranges obtained from the range tracker with errors $\bar{\varepsilon}_n$ and $\bar{\varepsilon}_o$ respectively. Define the delta range

$$\Delta\bar{R}_n = \bar{R}_n - \bar{R}_o \ .$$

Consequently the error $\delta\bar{R}_n$ of $\Delta\bar{R}_n$ is

$$\delta\bar{R}_n = (\bar{R}_n - R_n) - (\bar{R}_o - R_o) = \bar{\varepsilon}_n - \bar{\varepsilon}_o$$

The comparisons y_n can now be considered, where

$$y_n = \Delta\tilde{R}_n - \Delta\bar{R}_n .$$

Since, $\Delta\tilde{R}_n - \Delta\bar{R}_n = \delta\tilde{R}_n - \delta\bar{R}_n$

and $\delta\tilde{R}_n - \delta\bar{R}_n = \frac{\lambda}{2} f_r(t_n - t_o)\Delta N + \tilde{\varepsilon}(n) - \bar{\varepsilon}_n + \varepsilon_o$,

the comparison y_i ($i = 1, 2, \ldots, N$) can be expressed as

$$y_i = \beta_o + X_i\beta_1 + E_i \qquad (A.2)$$

where $\beta_o = \varepsilon_o$; $X_i = \frac{\lambda}{2} f_r(t_i - t_o)$; $\beta_1 = \Delta N$; and

E_i is a zero mean, serially uncorrelated random error with variance $\sigma^2 \cong$ variance of $\bar{\varepsilon}_i$.

For $n \geq 2$, with matrix notation, the least squares solution of (A.2) is

$$\begin{bmatrix} \hat{\beta}_o \\ \hat{\beta}_1 \end{bmatrix} = \left[\sum_{i=1}^{n} \begin{bmatrix} 1 & X_i \\ X_i & X_i^2 \end{bmatrix} \right]^{-1} \sum_{i=1}^{n} \begin{bmatrix} y_i \\ X_i\, y_i \end{bmatrix} .$$

The integer η for which the absolute value $\hat{\beta}_1 - \eta$ is minimum will be the estimate of ΔN from this example.

This page left intentionally blank.